

NATURE AND CANCELLATION OF STIMULUS ARTEFACT IN MOTOR-SENSORY EVOKED POTENTIALS - AN OVERVIEW

Prof. D.Sc. Ivan Assenov Dotsinsky, Eng. Agostinho Dos Santos
 Technical University of Sofia

The evoked potentials, emanating from the central and peripheral nervous system in response to external stimuli, are used for evaluation of suspected disorders affecting the skeletal muscles or the lower motor neuron. The excitation reaches the spinal cord through an afferent way and comes back to the muscle via efferent nerve. Usually, the conduction velocity of nerve and muscle fibers is measured (LEWIS and SUMNER, 1982; STÅLBERG and FALCK, 1993). Stimuli are applied consecutively in a proximal and a distal point along the nerve of the limb of interest (Fig. 1). The two responses are acquired, the corresponding latencies are measured and its difference is calculated (Fig. 2). The conduction velocity is obtained dividing the difference by the distance between the stimulating points. More sophisticated analysis may be performed using the distribution estimation of the fiber conduction velocities (McGILL *et al.*, 1982; STEGEMAN *et al.*, 1983).

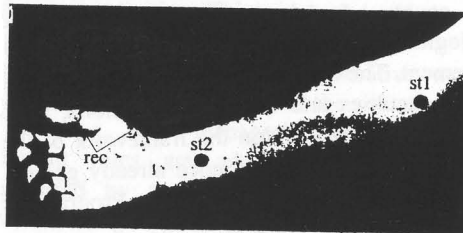


Fig. 1

The evoked potentials are mono- and bipolar (Fig. 2 and 3). Their amplitudes are in the μV range but may rarely reach 1 mV.

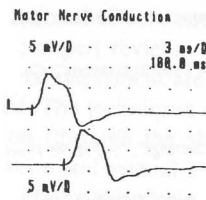


Fig. 2

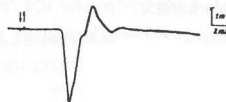


Fig. 3

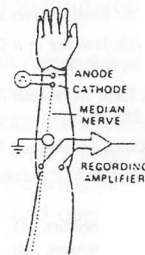


Fig. 4

The techniques implemented are two types: orthodromic, when the stimulus-response direction coincides with the normal excitation propagation and antidromic when these directions are opposite. The efferent nerve stimulation shown in Fig. 4 is antidromic while for an afferent nerve the stimulation is orthodromic.

Two types of electrodes are normally used in electromyography: needle and surface. The needle electrodes are inserted in the muscle and can acquire signals from one motor unit or from a few muscle fibers. The surface electrodes are atraumatic. They take signals from many units. Nevertheless, they are convenient in most motor nerve examinations.

The unwanted impedance of the interface between surface electrodes and subcutaneous tissue may be reduced by special paste. When a metal electrode comes in contact with an electrolyte, electron-to-ion exchange occurs leading to charge distribution. The boundary layer (of the order of the diameter of one or two water molecules) behaves as a capacity. In the absence of external electron source, an equilibrium potential is reached between the opposite oxidation and reduction reactions. If currents flow across the interface, new dynamic equilibrium is established. The resulting voltage drop is non-linearly related to the current.

Many models are developed to describe the properties of the electrode-electrolyte interface. The simplest is proposed by WARBURG (1899) and represents resistance R and capacitance C connected in series (Fig. 5a). However, these components are not typical because their values are not constant, but vary with both frequency and current density.

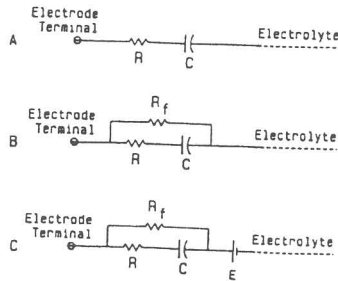


Fig. 5

The WARBURG circuit takes part in subsequent model improvements (RAGHEB and GEDDES, 1991; SCHWAN, 1992; MAYER *et al.*, 1992). A parallel Faradic resistance R_f is added to simulate the direct current passing through the electrodes (Fig. 5b). R_f is high in the low frequency region and is decreasing with an increase in current density. Finally, the equivalent circuit is completed with the half-cell potential E (Fig. 5c).

The processes in the electrode-skin-subcutaneous tissue interface are more expressed under the stimulating electrodes where the current density is highest. In addition, the field characteristics under anode and cathode differ slightly.

Stimulators with constant current or constant voltage output stages are used. The constant current stages are preferred, however most sophisticated combined versions have also been developed. Usually rectangular pulses with controlled amplitude and duration from 0.1 through 0.5 ms are used (STÅLBERG and FALCK, 1993). In order to activate all most rapidly conducting fibers in the nerve, the stimulus intensity is recommended to be at least 30% stronger than a supramaximal, which is found by increasing its strength until it has no further effect on the size of the evoked potential (LENMAN and RITCHIE, 1970). The maximal rate of stimulation is limited by the refractory period, immediately following the initiation of an action potential during which a second stimulus fails to evoke a second nerve response. The refractory period is about 0.6 ms (McGILL *et al.*, 1982).

The electrode polarization is a major nuisance because the potential difference may reach several hundred mV. Usually, an AC recording amplifier is used to reject the DC component from the acquired evoked potentials. However, the RC circuit enhances distortions, due to the interaction between stimulator, human body and amplifier.

Fig. 6 shows a multichannel time-constant free amplifier (DOTSINSKY *et al.*, 1991). The DC components are subtracted at the first stage outputs using a DAC controlled by a μP system. Modifications of this circuit may be used for evoked potential acquisition.

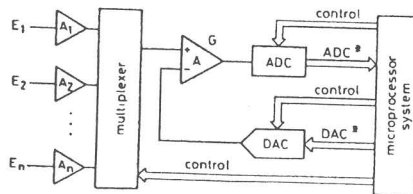


Fig. 6

The current injected between the stimulating electrodes flows through the tissues, setting up a potential field and contaminating the evoked potentials by an artifact. It consists of an initial spike and a longer lasting tail (Fig. 7). Some of the artefact sources are (McGILL *et al.*, 1982):

- *The voltage gradient under the recording electrodes.* Potentials measured at several points on the limb with respect to the ground electrode are shown in Fig. 8a. They are in the mV range but high enough for an artefact generation. The potential field suggests a ground electrode location near to the recording electrodes. A typical

voltage-time diagram of limb takeoff point can be seen in Fig. 8b. The end of the stimulus initiates an abrupt change in the exponential form of the potential due to the current through the ground electrode impedance. The arrow shows the time instant of measuring the potentials of Fig. 8a. Fig. 8c illustrates the voltage between two points not lying on an equipotential line.

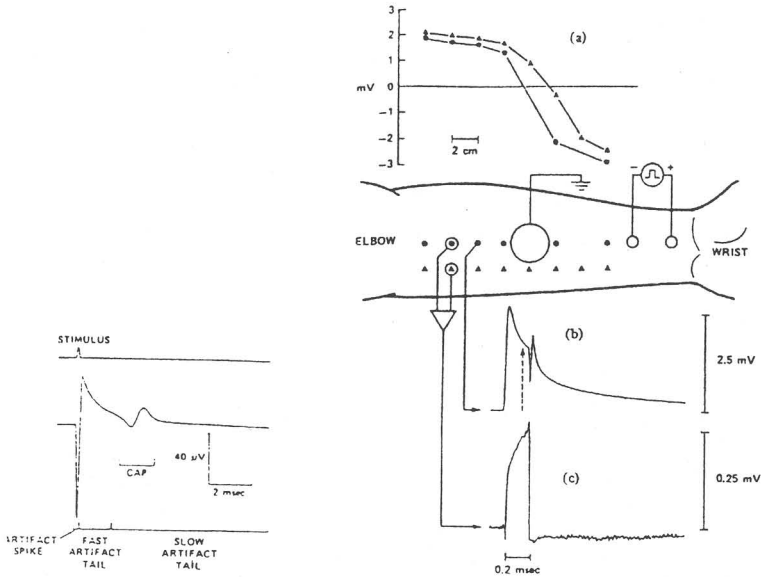


Fig. 7

Fig. 8

- *The parasitic capacitances between stimulator and amplifier.* The wires are usually not shielded in order to reduce the capacitance with respect to ground. Therefore, the capacitance between stimulating and recording wires may reach 0.5 pF even when they are well separated. The amplified parasitic signal depends on the imbalance of the electrode impedances that transforms the common mode interference in a false differential signal.

In summary, the artefact amplitude depends on the electrode configuration, the stimulus intensity, the type of the stimulator output stage and the properties of the amplifier input stage.

Some guidelines have been recommended to suppress the artefacts (McGILL *et al.*, 1982; NILSSON *et al.*, 1988; MINZLY *et al.*, 1993; KNAFLITZ and MERLETTI, 1998):

- Stimuli ‘isolation’ using screened transformer, radio frequency modulation or optical coupling.
- Electrode impedance reduction by skin abrasion.

- Positioning the recording electrodes on an equipotential line if possible.

Part of the influence of the artefact may be reduced by using a DC amplifier. Other hardware solutions are also proposed to artefact cancellation.

KNAFLITZ and MERLETTI (1988) designed a hybrid stimulator that generates constant current stimuli and switches to constant voltage mode during the rest intervals for faster discharge of electrode and tissue capacitances (Fig. 9).

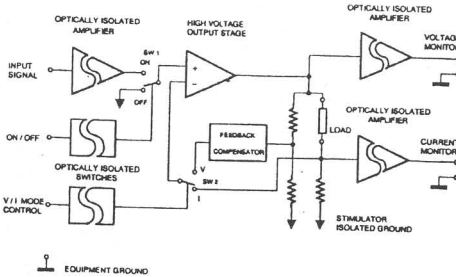


Fig. 9

MINZLY *et al.* (1993) proposed a suppressor that inhibits the amplifier input till an appropriate time-delay from the stimulus pulse is elapsed (Fig. 10). Thereby the artefact peak may be really blocked, but the muscle response will remain contaminated, as the tail can not be suppressed by any type of masking.

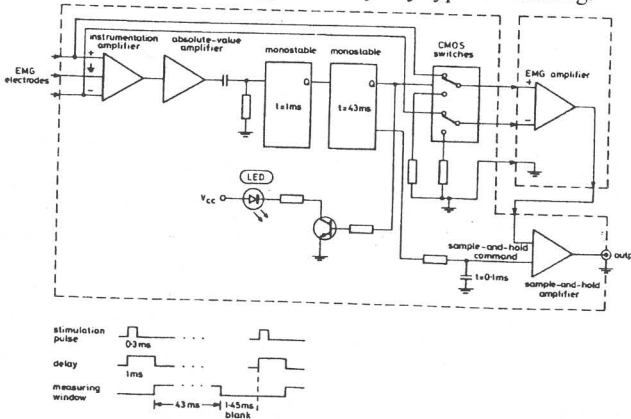


Fig. 10

One of the most efficient methods is the biphasic stimulation (NILSSON *et al.*, 1988). Two stimulating pulses are generated, the second after a short delay, falling in the muscle refractory period, thus evoking an artefact only. Both artefacts are mutually compensated to some extent, limited by their time-shift and the difference between

cathode and anode voltages, even with stimuli with identical intensity. Still, the method offers a relatively free of distortion muscle response. Fig. 11 presents recordings of surface antidromic mono- and biphasic stimulation of the sural nerve.

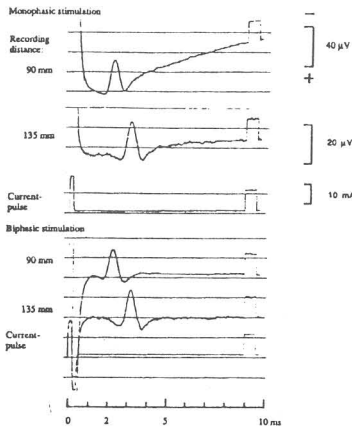


Fig. 11

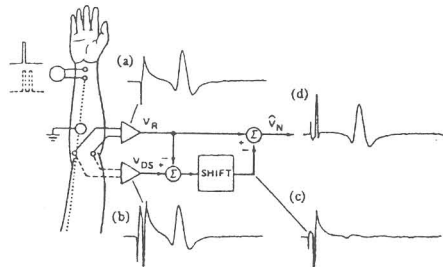


Fig 12

Recently, various software approaches are implemented. The double-stimulus method is similar to the biphasic one (Fig. 12). Two potentials are recorded in sequence. The first is evoked by a single stimulus and the second - by two closely time-locked monophasic pulses that give rise to a double artefact. The potentials are subtracted to yield a single artefact, which is aligned with and subtracted from the first response. The inconvenience is that the two artefacts may differ considerably.

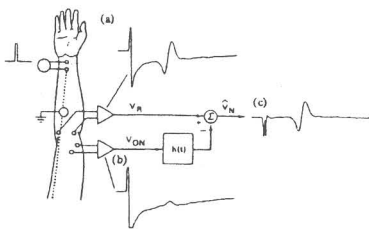


Fig. 13

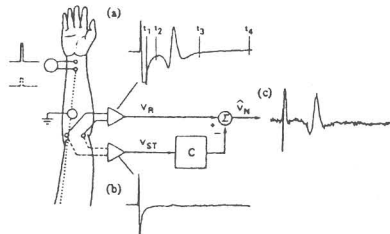


Fig. 14

The off-nerve method uses additional acquiring electrodes situated away from the muscle (Fig. 13). Nevertheless, the two artefacts are not linearly related and the nerve response is usually estimated by some kind of weighting function. Moreover, it is very difficult to find electrode locations that might be completely free of evoked signal.

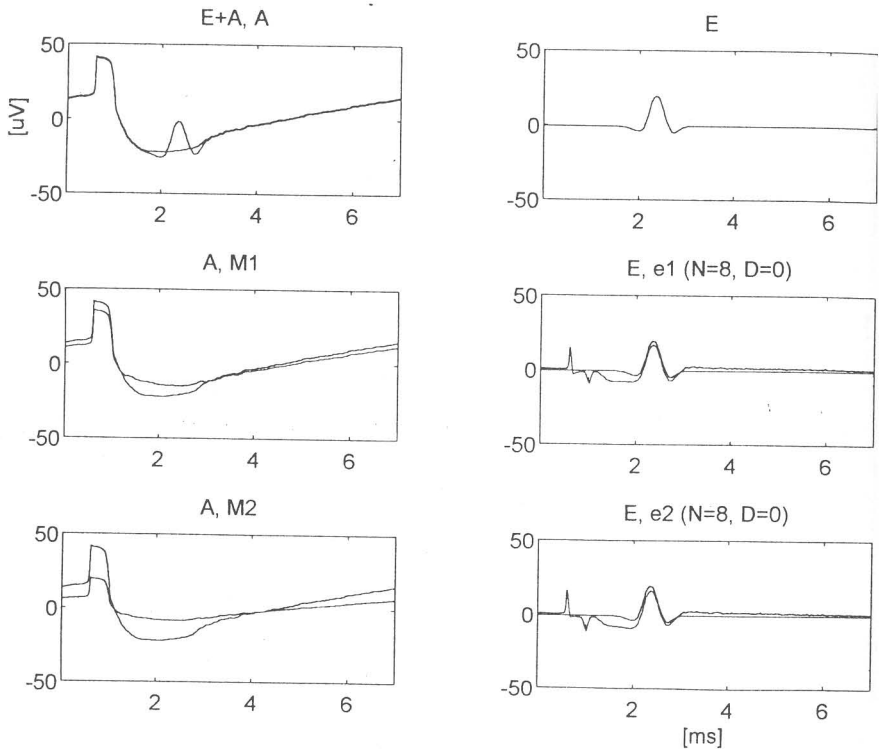


Fig. 15

The subthreshold method uses a second recording with reduced stimulus intensity that does not provoke excitation (Fig. 14). The first recording is a contaminated evoked signal, while the second is a ‘pure’ artefact. Since the subthreshold artefact has a very low amplitude, it is scaled before subtraction from the contaminated signal. However, many stimuli are required to average out the noise (McGILL *et al.*, 1982).

The subtraction methods (double-stimulus, off-nerve and subthreshold) are based on the presumption of an available ‘pure’ artefact for subtraction that is never entirely true. An alternative way is found in adaptive filtration, where these artefacts are supplied to the reference input of an adaptive filter (DOS SANTOS *et al.*, 1997). A selected contaminated signal $E+A$ (where E is the evoked potential and A is the artefact) was concatenated to form a repetitive sequence, presented at the primary input of the filter (left upper part of Fig. 15). A was visually extracted by splitting $E+A$ in two separate signals. The right upper diagram presents the muscle response E , which is taken further and considered as a ‘pure’ action potential. Then A is modified in amplitude and shape and the resulting signal M is led to the reference input of the filter. The left middle part of Fig. 15 depicts A and M_1 - obtained by introducing small variation in the shape and 10% reduction of amplitude (dashed line). The diagram below shows a similar signal M_2 with lower amplitude (50% reduction) and higher distortion in shape. The right middle diagram shows the ‘pure’ evoked potential E together with the filtered signal e_1 (dashed line), using M_1 as a reference signal. The right lower diagram presents the result with M_2 taken as a reference signal. A causal filter (time-delay between the input signals $D=0$) with small number of Widrow coefficients $N=8$ was found optimal for eliminating the time shift. The resulting DC shift is without any influence on the shapes of e_1 and e_2 , which are virtually identical with the response waveform, except for the initial part, where a small depression seems to be quite tolerable. No other non-linear shape changes in the filtered evoked potential can be observed.

Encouraging results in artefact cancellation are obtained by exponential approximation of the contaminated signal (DOTSINSKY *et al.*, in press). A contaminated evoked signal $c(t)$ is shown in Fig. 16a. Some signal samples and thresholds are detected : **sig_max**, **sig_min**, **sig_avg**, **hi_thresh** and **low_thresh**. A mark **beg_pulse** is assigned to the location where for the first time the current sample is either higher than **hi_thresh** or lower than **low_thresh**. The location **end_pulse** is recognized in a next sample that crosses back the corresponding threshold. The turning point following **end_pulse** is marked as **end_spike**. Then the artefact is approximated by two overlapping exponential parts: $a_1(t)$ for the spike trailing edge and another $a_2(t)$ for the tail of the artefact. They are subtracted consecutively from $c(t)$ to yield a ‘pure’ action potential $p(t)$.

$$c_1(t) = c(t) - a_1(t) \text{ for } t \in [\text{end_pulse}, \text{end of the signal}].$$

$$c_2(t) \equiv p(t) = c_1(t) - a_2(t) \text{ for } t \in [\text{end_spike}, \text{end of the signal}].$$

The result of the approximation procedure applied on the contaminated signal from Fig. 16a is presented in Fig. 16b, where an adequate artefact cancellation can be seen.

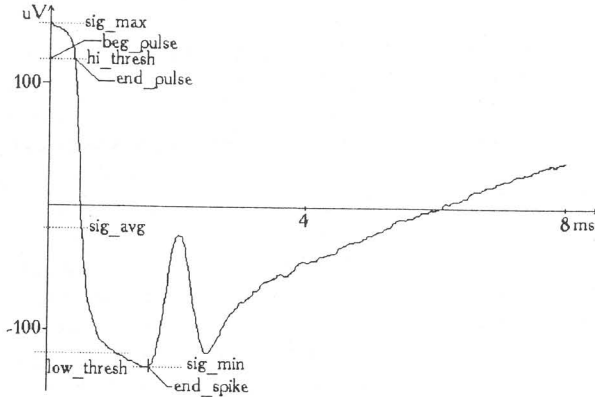


Fig. 16a

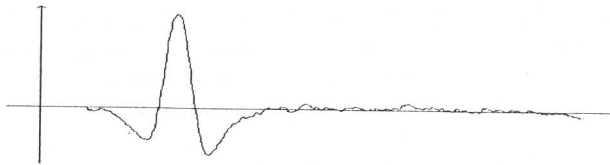


Fig. 16b

References

1. BUCHTAL F. and ROSENFALK A. (1966): 'Evoked action potentials and conduction velocity in human sensory nerves', *Brain Res.*, **3**, pp. 1-122
2. DOS SANTOS A., TASHEV I. and DOTSINSKY I. (1997): 'Artefact suppression in nerve evoked signals using adaptive filtering', *Proceedings of the Conference with International Participation "ELECTRONICS - ET'97"*, Sozopol, **1**, pp.145-150
3. DOTSINSKY I.A., CHRISTOV I.I., DASKALOV I.K. (1991): 'Multichannel DC amplifier for a microprocessor electroencephalograph', *Med. Biol. Eng. Comput.*, **29**, pp. 324-329
4. DOTSINSKY I., DOS SANTOS A. and TASHEV I. (in press): 'Artefact cancellation in motor-sensory evoked potentials: two approaches using adaptive filtration and exponential approximation', *Med. Biol. Eng. Comput.*
5. KNAFLITZ M. and MERLETTI R. (1998): 'Suppression of Stimulation Artifacts from Myoelectric-Evoked Potential Recordings', *IEEE Trans. on Biomed. Eng.*, **35**, No 9, pp. 758-763

6. LENMAN J.A.R. and RITCHIE A.E. (1970): 'Clinical Electromyography', *Pitman Medical Scientific Publ. C.L., GB*.
7. LEWIS A.H. and SUMNER A.J. (1982): 'Electrodiagnostic distinctions between chronic familial and acquired demyelinating polyneuropathies', *Neurology*, **32**, pp. 592-596
8. MAYER S., GEDDES L.A., BOURLAND J.D. and OGBORN L. (1992): 'Electrode Recovery Potential', *Ann. Biomed. Engng.*, **20**, pp. 385-394
9. MCGILL K.C., CUMMINS K.L., DORFMAN L.J., BERLIZOT B.B., LUETKEMEYER K., NISHIMURA D.G., and WIDROW B. (1982): 'On the Nature and Elimination of Stimulus Artifact in Nerve Signals Evoked and Recorded Using Surface Electrodes', *IEEE Trans. on Biomed. Eng.*, **29**, No 2, pp. 129-136
10. MINZLY J., MIZRAHI J., HAKIM N. and LIBERSON A. (1993): 'Stimulus artefact suppressor for EMG recording during FES by a constant-current stimulator', *Med. Biol. Eng. Comput.*, **31**, pp. 72-75
11. NILSSON J., RAVITS L. and HALLET M. (1988): 'Stimulus Artefact Compensation using Biphasic Stimulation', *Muscle Nerve*, **11**, pp. 597-602
12. PARSA V., PARKER P.A. and SCOTT R.N. (1998a): 'Adaptive Stimulus Artifact Reduction in Noncortical Somatosensory Evoked Potential Studies', *IEEE Trans. on Biomed. Eng.*, **45**, No 2, February, pp. 165-179
13. PARSA V., PARKER P. and SCOTT R. (1998b): 'Convergence characteristics of two algorithms in non-linear stimulus artefact cancellation for electrically evoked potential enhancement', *Med. Biol. Eng. Comput.*, **36**, March, pp. 202-214
14. SCHWAN H.P. (1992): 'Linear and Nonlinear Electrode Polarization and Biological Materials', *Ann. Biomed. Engng.*, **19**, pp. 269-288
15. RAGHEB T. and GEDDES L.A. (1991): 'The polarization Impedance of Common Electrode Metals Operated at Low Current Density', *Ann. Biomed. Engng.*, **19**, pp. 151-163
16. STÅLBERG E. and FALCK B. (1993): 'Clinical Motor Nerve Condition Studies', *Meth. Clin. Neurophysiol.*, **4**, pp. 61-80
17. STEGEMAN D.F., DE WEERD J.P.C. and NOTERMANS S.L.H. (1983): 'Modelling compound action potentials of peripheral nerves in SITU. III. Nerve propagation in the refractory period', *Electroenceph. Clin. Neurophysiol.*, **55**, pp. 668-679